Cognitive, structural and microstructural changes in presymptomatic carriers of *c9orf72* mutation

Anne Bertrand, MD, PhD[1,2*], Junhao Wen, MS[2,3*], Daisy Rinaldi, PhD[1], Marion Houot[4], Sabrina Sayah[6] , Agnès Camuzat, PhD[5], Clémence Fournier, PhD[5] ; Sabrina Fontanella, MS[2,3], Alexandre Routier, MS[2,3], Philippe Couratier, MD[7], Florence Pasquier, MD PhD[8,9], Marie-Odile Habert[10], Didier Hannequin, MD, PhD[11,12], Olivier Martinaud, MD, PhD[11,12], Stanley Durrleman, PhD[2,3], Alexis Brice, MD[1], Olivier Colliot, PhD[1,2], Isabelle Le Ber, MD, PhD[1] and PREVDEMALS Study Group.

[1] Sorbonne Universités, UPMC Univ Paris 06, Inserm, CNRS, Institut du cerveau et la moelle (ICM), AP-HP - Hôpital Pitié-Salpêtrière, Paris, France; [2] Inria Paris, Aramis project-team, Paris, France; [3] Sorbonne Universités, UPMC Univ Paris 06, Inserm, CNRS, Institut du cerveau et la moelle (ICM) - Hôpital Pitié-Salpêtrière, Paris, France; [4] Institute of Memory and Alzheimer's Disease (IM2A), Centre of excellence of neurodegenerative disease (CoEN), ICM, APHP Department of Neurology, Hopital Pitié-Salpêtrière, University Paris 6, Paris, France; [5] Institut du cerveau et la moelle (ICM), Paris, France; [6] Center for Clinical Investigation (CIC), Institut du cerveau et la moelle (ICM), Paris, France; [7] Limoges University, Limoges, France; [8] INSERM U1171, National reference center for young onset dementia, Neurology department, University Hospital, Lille, France; [9] Lille University, Lille, France; [10] Department of Nuclear Medicine, AP-HP - Hôpital Pitié-Salpêtrière, Paris, France.; [11] CNR-MAJ / Rouen University Hospital, Rouen, France; [12] CHU Rouen, Rouen, France .

- *c9orf72* mutation, identified in 2011, represents the first cause of genetic **frontotemporal lobar degeneration** (FTLD) and **amyotrophic lateral sclerosis** (ALS)[1,2].
- **Recent preclinical development of disease-modifying drugs**, such as antisense oligonucleotides that target mutant RNA, or small molecules that counteract mutant RNA pathogenic effects, offer promising therapeutic perspectives in *c9orf72* disease[3,4].
- Because neurodegenerative diseases progress during decades before the onset of clinical symptoms[5], **presymptomatic carriers represent an optimal target population for therapeutic trials**, as they offer an early therapeutic window.
- **Identification of biomarkers in presymptomatic subjects is thus critical**, in order to monitor the effects of disease-modifying drugs during future trials.

• Methods

- **Subjects**: 80 neurologically healthy participants were included in a national multicentric study (PrevDemAls study) between 2015 and 2017. The participants were first degree relatives of *c9orf72* patients or mutation carriers, who had 50% risk to carry a *c9orf72* expansion.
- **Genetic analysis**: *c9orf72* genetic status was determined by repeat-primed-PCR on DNA of peripheral lymphocytes; southern-blot was done in expansion carriers to accurately determine the size of the expansion. Forty-one asymptomatic participants carried a pathogenic *c9orf72* repeat expansion (mean expansion size: 2379 GGGGCC repeats, range: 309 to 3286 repeats). Thirty-nine participants that did not carry pathogenic expansion (<23 GGGGCC repeats) were considered as a control group. The expected ages at onset of *c9orf72* mutation carriers were estimated by averaging the age at onset of affected relatives in the family.
- **Neuropsychological tests**: All the participants underwent a comprehensive neuropsychological battery and behavioral evaluation. Global cognitive efficiency was assessed using the Mini Mental State Examination (MMSE)[6] and the MATTIS dementia rating scale[7]. Executive functions were assessed with the Frontal Assessment Battery (FAB)[8], and social cognition using the Social Cognition and Emotional Assessment test (SEA), which includes (1) the Emotion Recognition test (scored from 0 to 15) in which patients must identify which emotion is being expressed, and (2) the Faux Pas recognition test (scored from 0 to 15) that evaluates theory of mind[9]. Episodic memory was assessed using the Free and cued recall test[10]. Praxis were assessed using copy and recall at 15 min of the Benson figure[11] and a shortened version of the Batterie d'Evaluation des Praxie [12] with six testing conditions : (a) manual dexterity, (b) melokinetic apraxia, (c) imitation of non-representational gestures, (d) pantomime of intransitive gestures, (e) pantomime of transitive gestures. Neurological examination and neuropsychological tests were performed by a Neurologist (ILB) and a Neuropsychologist (SS) blind from the genetic status of participants.
- **MRI acquisition**s were performed on a 3T MR system (Siemens Prisma 3T for 64 subjects; Philips Achieva 3T for 9 subjects; GE 3T for 7 subjects). Parameter of 3DT1 sequence were as follow: field of view = 282x282mm; matrix size = 256x256; slice thickness= 1.1mm; spatial resolution = (1.1x1.1x1.1) mm^3; TE = 2.8-3ms; TR = minimum; Bandwidth: 240-255 Hz; Flip angle: 8°. The 67 subjects imaged on a Siemens Prisma MR also underwent DTI with the following parameters: field of view = 192x192mm; matrix size = 96x96; slice thickness= 2.5mm; spatial resolution = (2x2x2.5) mm3; TE = 90ms; TR = 7300ms; Bandwidth = 1580 Hz. One hundred thirty-seven separate images were acquired for each DTI scan: 64 diffusion-weighted images (b value = 1000 s/mm2) and 9 T2-weighted images with no dedicated diffusion sensitization (b value = 0 s/mm2). A B0 field map was also acquired in order to correct for geometrical distortions induced by the EPI technique.
- **Structural MRI processing**: FreeSurfer image analysis (stable version 5.3; http://surfer. nmr.mgh.harvard.edu) software was used to process the T1-weighted images. Briefly, the processing pipeline included non-uniformity and intensity correction, skull stripping, grey/white matter segmentation, reconstruction of the cortical surface and segmentation of cortical structures. We used the Desikan atlas to estimate the volume (in mm^3) of cortical ROI (supplementary table 2). We also extracted the volume of 18 subcortical grey matter ROI (right and left cerebellum, ventral diencephalon, putamen, pallidum, caudate, accumbens, amygdala, thalamus and hippocampus), and the total intracranial volume (TIV). We used for analyses the normalized volume of each ROI, defined as NVROI = (TIVm.VROI)/TIV, where TIVm is the average total intracranial volume computed across all participants, which is constant, and VROI is the volume of the ROI. The role of the constant multiplicative factor TIVm is simply to preserve the order of magnitude of NVROI similar to that of VROI.
- **DTI processing**: For each subject, all raw DWI volumes were aligned to the average b0 image and corrected for eddy current distortions using the FSL flirt tool (www.fmrib.ox.ac.uk/fsl). To correct for echo-planar imaging (EPI) induced susceptibility artifacts, the field map image was used as proposed by Jezzard & Balaban[13] with the FSL prelude/fugue tools. Finally, the DWI volumes were corrected for nonuniform intensity using ANTs N4 bias correction algorithm[14]. A single multiplicative bias field from the averaged b0 image was estimated[15]. The DWI datasets were up-sampled at 1mm in order to improve the registration between the T1-weighted image and the DWI. A diffusion tensor model was fitted at each voxel to calculate Fractional Anisotropy (FA), Mean Diffusivity (MD), Radial Diffusivity (RD) and Axial Diffusivity (AD) maps. White matter tracks were defined using the JHU white-matter tractography atlas[16]. For each subject, the FA map was registered onto the FA map of the JHU atlas template with the ANTs SyN algorithm[17]. Then, the estimated non-linear deformation was applied to the MD, RD and AD maps so that all maps of each individual were put into correspondence with the JHU atlas. Then we extracted, in each patient, the average values of DTI metrics (FA, MD, RD and AD) within each tract of the JHU atlas.
- **Statistical analysis**: Statistical analyses were performed using R 3.4.0 (The R Foundation for Statistical Computing, Vienna, Austria) and GraphPad Prism 7.0 (La Jolla, CA, USA). Structural and microstructural differences between carriers and non-carriers of the c9orf72 mutation were assessed using linear mixed-effects models, with both fixed and random effects, using the following model: $Y_i^{(J)} = \mu + \beta \times gender_i + \lambda \times age_i + \eta \times group_i + U_i + \epsilon_i^{(J)}$ where $Y_i^{(J)}$ is the response of the j^{th}region of interest (ROI) for the i^{th} subject; $gender_i$, age_i, and $group_i$ are the fixed effects; μ, β, λ and η are the estimated parameters; U_i is the kinship-specific random effect measuring the difference between the average response in the family and in the whole population; $\epsilon_i^{(J)}$ is the observation error.

• Results

- *c9orf72* mutation is associated with **subtle praxis impairment**

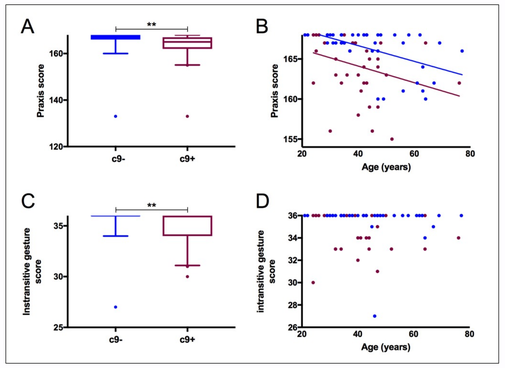

- *c9orf72* mutation is associated with **diffuse cortical atrophy**, sparing frontobasal regions and primary motor cortex

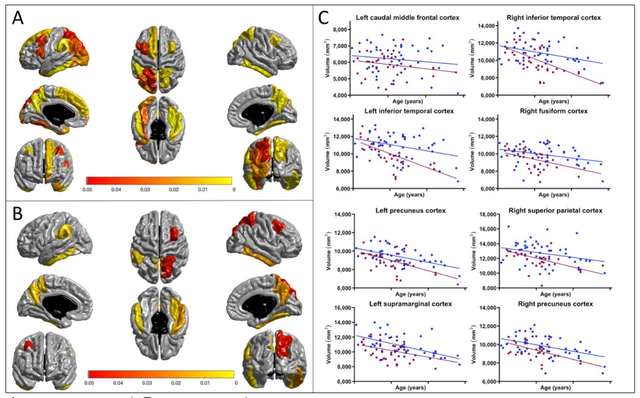

A: uncorrected, B: corrected

- *c9orf72* mutation is associated with **thalamic atrophy**

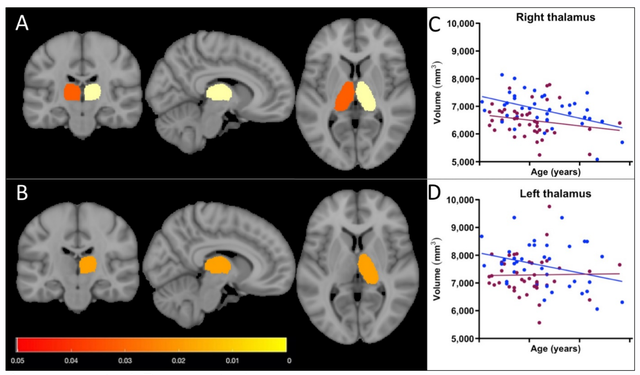

A: uncorrected, B: corrected

- *c9orf72* mutation is associated with **alterations of white matter microstructure**, predominating in frontal lobes and corticospinal tracts

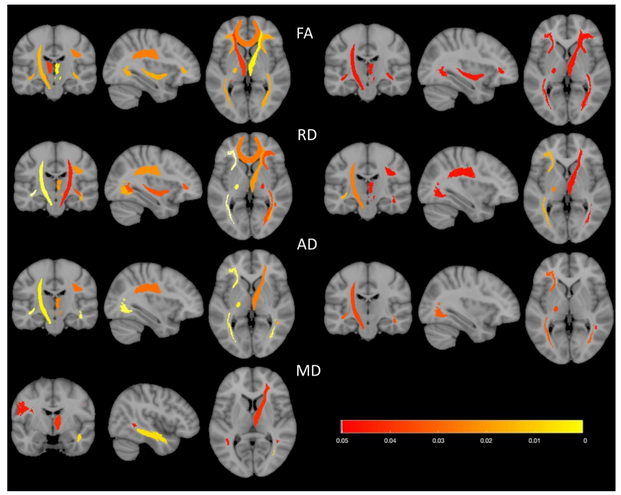

• Discussion & conclusions

- **Praxis impairment** was present in young subjects carrying *c9orf72* mutation. This result is unexpected, as praxis alterations are usually not the most salient feature of c9orf72 FTLD[8–22]. It may represent an early-expressed and non-evolving endophenotype of c9orf72 mutation.
- Our study demonstrates **differences of pattern between cortical atrophy and white matter alteration in c9+ subjects**. Cortical atrophy appears widespread, with a relative sparing of primary motor cortex and frontobasal cortex, both areas that are preferentially involved during ALS and FTLD. Oppositely, white matter alterations seem to target preferentially both the corticospinal tracts and white matter tracts connected to the frontal lobes. This suggest that white matter changes are likely more predictive of future cognitive and motor deficits. These differences are reminiscent of the distinct topography of the 2 histopathological hallmarks of c9orf72 mutation, DPR deposits and TDP-43. DPR deposits have a diffuse repartition within cortical, subcortical and cerebellar regions; they appear unrelated to the clinical phenotype of patients, whileTDP-43 deposits are more correlated to clinical symptoms[23–26]. We hypothesize that the diffuse atrophy process in c9+ relates more to the effect of DPR, while white matter changes relates more to TDP-43 pathology.
- **Thalamic atrophy** has been previously reported in smaller cohorts of presymptomatic c9orf72 carriers[27–29], and also in symptomatic c9orf72 carriers with FTLD[21,30,31] or ALS[32]. Thalamic atrophy may be related to the local presence of pathological deposits, i.e. TDP-43 and/or DPR deposits, but it can also be related to deafferentation processes secondary to the diffuse cortical atrophy, due to the high number of connection between the hemispheric cortex and the thalamus. These mechanisms are not exclusive and may be associated. For these reasons, and because of its easy segmentation, the thalamus represents a promising biomarker of early structural changes in c9orf72 mutation carriers.

• References

1. DeJesus-Hernandez M, Mackenzie IR, Boeve BF, et al. Neuron. 2011;72:245–256.
2. Renton AE, Majounie E, Waite A, et al. Neuron. 2011;72:257–268.
3. Donnelly CJ, Zhang P-W, Pham JT, et al. Neuron. 2013;80:415–428.
4. Jiang J, Zhu Q, Gendron TF, et al. GNeuron. 2016;90:535–550.
5. Bateman RJ, Xiong C, Benzinger TLS, et al. N Engl J Med. 2012;367:795–804.
6. Folstein MF, Folstein SE, McHugh PR. J Psychiatr Res. 1975;12:189–198. 7
7. Mattis S. Geriatr Psychiatry Handb Psychiatr Prim Care Physicians. New York: Grune & Stratton; 1976.
8. Dubois B, Slachevsky A, Litvan I, Pillon B. Neurology. 2000;55:1621–1626.
9. Funkiewiez A, Bertoux M, de Souza LC, Lévy R, Dubois B. Neuropsychology. 2012;26:81–90.
10. Grober E, Buschke H, Crystal H, Bang S, Dresner R. Neurology. 1988;38:900–903.
11. Possin KL, Laluz VR, Alcantar OZ, Miller BL, Kramer JH. Neuropsychology. 2011;49:43–48.
12. Peigneux P, Van Der Linden M. Rev Neuropsychol. 2000;10:311–362.
13. Jezzard P, Balaban RS. Magn Reson Med. 1995;34:65–73.
14. Tustison NJ, Avants BB. Front Neuroinformatics. 2013;7:39.
15. Jeurissen B, Tournier J-D, Dhollander T, Connelly A, Sijbers J. NeuroImage. 2014;103:411–426.
16. Mori S, Wakana S, Nagae-Poetscher L, van Zijl P. Amsterdam: Elsevier; 2005.
17. Avants BB, Epstein CL, Grossman M, Gee JC. Med Image Anal. 2008;12:26–41.
18. Devenney E, Hornberger M, Irish M, et al. JAMA Neurol. 2014;71:331.
19. Floeter MK, Traynor BJ, Farren J, et al. Neurology. Epub 2017 Jun 14;10.1212.
20. Mahoney CJ, Beck J, Rohrer JD, et al. Brain. 2012;135:736–750.
21. Sha SJ, Takada LT, Rankin KP, et al. Neurology. 2012;79:1002.
22. Suhonen N-M, Haanpää M-R, Korhonen V, et al. J Alzheimers Dis. 2017;58:479–489.
23. Davidson Y, Robinson AC, Liu X, et al. Neuropathol Appl Neurobiol. 2016;42:242–254.
24. Davidson YS, Barker H, Robinson AC, et al. Acta Neuropathol Commun. 2014;2:70.
25. Gomez-Deza J, Lee Y-B, Troakes C, et al. Acta Neuropathol Commun. 2015;3:38.
26. Mackenzie IRA, Frick P, Grässer FA, et al. Acta Neuropathol (Berl). 2015;130:845–861.
27. Lee SE, Sias AC, Mandelli ML, et al. Neuroimage Clin [online serial]. Epub 2016 Dec.
28. Rohrer JD, Nicholas JM, Cash DM, et al. Lancet Neurol. 2015;14:253–262.
29. Walhout R, Schmidt R, Westeneng H-J, et al. Neurology. 2015;85:1780–1788.
30. Floeter MK, Bageac D, Danielian LE, Braun LE, Traynor BJ, Kwan JY. NeuroImage Clin. 2016;12:1035–1043.
31. Mahoney CJ, Beck J, Rohrer JD, et al. FBrain. 2012;135:736–750.
32. Agosta F, Ferraro PM, Riva N, et al. Neurobiol Aging [online serial]. Epub 2017 Jun.